

Intraband optical conductivity $\sigma(\omega, T)$ of Cu, Ag, and Au: Contribution from electron-electron scattering

G. R. Parkins, W. E. Lawrence, and R. W. Christy

Department of Physics and Astronomy, Dartmouth College, Hanover, New Hampshire 03755

(Received 4 December 1980)

The intraband optical conductivity of all the noble metals has been measured at the temperatures 77, 295, and 425 K. In all cases the Drude scattering rate $\tau^{-1} = \alpha(T) + \beta(\hbar\omega)^2$ for $\hbar\omega$ less than about 2 eV. The temperature-dependent intercept $\alpha(T)$ may be attributed to electron-phonon scattering. The quadratic dependence on ω , with β found to be temperature independent, is suggestive of electron-electron scattering. However, the observed values of β exceed current theoretical estimates by a factor of 2 or 3. Moreover, β should be related to the dc electrical and thermal resistivities (in the limited temperature regimes in which electron-electron scattering contributes appreciably). If this comparison is made, the discrepancy worsens to an order of magnitude. We briefly discuss other mechanisms which might account for the large observed values of β , but none looks sufficient. We conclude that the frequency dependence in the Drude scattering rates of the noble metals, while qualitatively suggestive of electron-electron scattering, is quantitatively not understood.

I. INTRODUCTION

The optical properties of the noble metals at photon frequencies below the interband absorption edge can be explained by simple Drude theory, if a frequency-dependent scattering rate $1/\tau$ is assumed. Using our present room-temperature data on Cu and Ag, Beach and Christy¹ developed a model for $1/\tau$ in which the scattering rate was considered to be made up of three independent components: one due to electron-phonon scattering that is temperature dependent but photon-energy independent, one due to electron-electron scattering that is temperature independent, and one due to electron-defect scattering. In this paper we extend the earlier analysis¹ to include our new results for Au, as well as our new results for all three metals above and below room temperature. We will show that these new experimental data² exhibit the temperature dependences expected on the basis of the model considered earlier. Moreover, the effects are scaled appropriately in Au, as compared with the other noble metals. However, the existence of new dc electrical-resistivity data,³ further analysis⁴ of thermal-resistivity data, and recent basic theoretical work,⁵⁻⁸ allow for a more thorough assessment of electron-electron scattering than made previously. This leads us to conclude that our observed frequency dependence cannot be accounted for on the basis of electron-electron scattering alone, within the framework of our current theoretical understanding.

According to Drude free-electron theory, the complex dielectric function is given by

$$\epsilon(\omega) = 1 - \frac{\omega_p^2}{\omega(\omega + i/\tau)}, \quad (1)$$

where the plasma frequency is

$$\omega_p^2 = \frac{4\pi ne^2}{m^*}, \quad (2)$$

n being the density and m^* the optical effective mass of the electrons. For noble metals in the near infrared $\omega\tau \gg 1$. Further, the large interband absorption peaks in the visible and uv have a significant effect on ϵ_1 at lower frequencies ($\epsilon \equiv \epsilon_1 + i\epsilon_2$), which takes the form of an added real constant term $\delta\epsilon_1$. Thus, we assume

$$\epsilon_1 = 1 + \delta\epsilon_1 - \frac{\omega_p^2}{\omega^2}, \quad \epsilon_2 = \frac{\omega_p^2}{\omega^3\tau}. \quad (3)$$

We have to determine $\delta\epsilon_1$, ω_p , and τ from the optical measurements, and then analyze the frequency and temperature dependence of τ .

Like Beach and Christy, we neglect the defect-scattering contribution to $1/\tau$. (Surface scattering is included by a correction to the reflectance data.) We take the theoretical phonon contribution from Holstein's results.^{9,10} For the frequencies of interest this depends only on temperature, and we write it as

$$\frac{1}{\tau_{ep}(\omega, T)} = \alpha(T). \quad (4)$$

The theoretical electron-electron contribution to $1/\tau$ we take as

$$\frac{1}{\tau_{ee}(\omega, T)} = \frac{\pi^3\Gamma\Delta}{12\hbar E_F} \left[(k_B T)^2 + \left(\frac{\hbar\omega}{2\pi} \right)^2 \right]. \quad (5)$$

The temperature and frequency dependences were derived by Gurzhi,¹¹ and the derivation of the numerical coefficient will be described in Sec. III. The dimensionless parameters Γ and Δ were defined in Ref. 12; briefly, Δ is the fractional

TABLE I. Experimental values of $\delta\epsilon_1$ at three different temperatures.

| | 78 K | 295 K | 425 K |
|----|------|-------|-------|
| Cu | 5.18 | 4.93 | 4.77 |
| Ag | 1.23 | 1.71 | 1.63 |
| Au | 4.82 | 4.44 | 4.34 |

umklapp scattering, and

$$\Gamma = (2k_F)^{-1} \int_0^{2k_F} dq \left(\frac{V_{ea}(q)}{\frac{2}{3} E_F} \right)^2$$

is the (dimensionless) averaged scattering probability. The temperature term in (5) is negligible compared either to $\alpha(T)$ or to $(\hbar\omega/2\pi)^2$ for optical frequencies, and thus we may write theoretically

$$1/\tau = \alpha(T) + \beta\hbar^2\omega^2, \quad (6)$$

where β is independent of T . In the next section the data are analyzed according to (6) and compared directly with theory. We indeed find β to be independent of T , but a factor of 2 or 3 larger than predicted for each metal. In Sec. III we discuss the theoretical relationships between β and the dc transport coefficients. These relationships are then used in Sec. IV to compare our measured β values with electrical- and thermal-resistivity data on the noble metals. Values of β inferred from dc measurements turn out to be about an order of magnitude less than our measured ones. Further recent theoretical calculations are also discussed in Sec. IV. In Sec. V we discuss other possible mechanisms for our observed frequency dependence and elaborate our conclusions.

II. RESULTS

The experimental details of the optical measurements have been described previously.^{1,2,13} Our data analysis that leads to the experimental values of $1/\tau$ was exactly the same as that of Beach and Christy,¹ except that we treated surface scattering more accurately by iteratively using Eq. (10a) of Ref. 1. Our values of $\delta\epsilon_1$ and ω_p are listed in Tables I and II, respectively. The results for

TABLE II. Experimental values of plasma frequency $\hbar\omega_p$ (eV).

| | 78 K | 295 K | 425 K |
|----|------|-------|-------|
| Cu | 8.89 | 8.82 | 8.79 |
| Ag | 8.86 | 8.97 | 8.97 |
| Au | 8.74 | 8.68 | 8.65 |

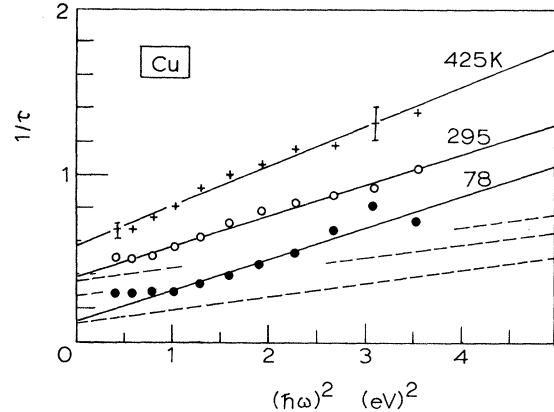


FIG. 1. Electron-scattering rate for copper in units of 10^{14} s^{-1} vs photon energy squared for three different temperatures. Solid line: least-squares fit to data (Ref. 2). Dashed line: calculated from theory, Eqs. (4)–(6).

$1/\tau$ at three different temperatures are shown by the points in Figs. 1–3 for Cu, Ag, and Au, respectively. The error bars shown are representative of the instrumental uncertainty. The solid lines are least-squares fits to the experimental points, and their intercepts and slopes are given in Tables III and IV, respectively.

The dashed lines in Figs. 1–3 are theoretical predictions based on volume-scattering mechanisms due only to electron-phonon and electron-electron interactions. The parameters used in Holstein's formula for $\alpha(T)$ and in Eq. (5) are those that were listed in Table I of Ref. 1. The intercepts and slopes of the dashed lines are given in Tables III and IV, respectively, for comparison with the experimental values.

The values of $\delta\epsilon_1$ in Table I are essentially independent of temperature, to within the ex-

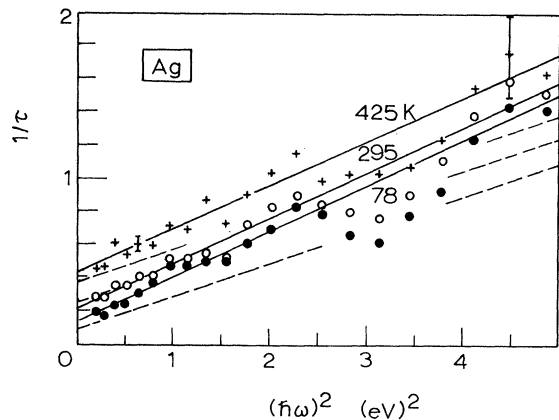


FIG. 2. Electron-scattering rate for silver in units of 10^{14} s^{-1} vs photon energy squared for three different temperatures. Solid line: least-squares fit to data (Ref. 2). Dashed line: calculated from theory, Eqs. (4)–(6).

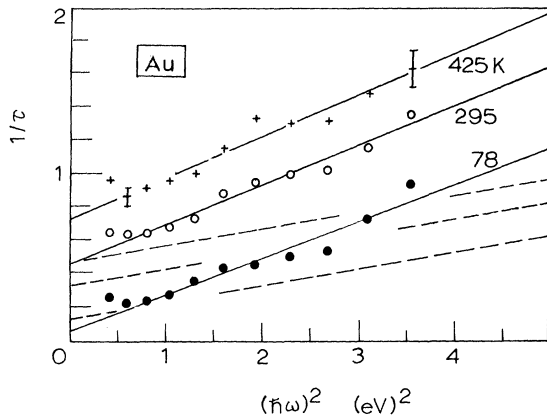


FIG. 3. Electron-scattering rate for gold in units of 10^{14} s^{-1} vs photon energy squared for three different temperatures. Solid line: least-squares fit to data (Ref. 2). Dashed line: calculated from theory, Eqs. (4)–(6).

perimental error, as might be expected from the Kramers-Kronig relation, since the temperature dependence of the interband ϵ_2 in the visible and w is slight. The apparent small decrease in Cu and Au may be real, however, in agreement with an overall decrease² of the interband ϵ_2 . The plasma frequencies in Table II are also nearly independent of temperature. The apparent decrease in Cu and Au is about what would be expected from the decrease of n in Eq. (2) due to thermal expansion, assuming that m^*/m is constant, with average values 1.505 and 1.076, respectively. The trend in Ag is opposite, however, and would imply optical masses of 1.038, 1.002, and 0.993 at the three increasing temperatures, although it could be due simply to experimental error. It is difficult to say what temperature dependence of m^* would be expected theoretically.

The intercepts $\alpha(T)$ ($=1/\tau_{e\phi}$) in Table III increase strongly with temperature, as expected theoretically if they are due primarily to electron-phonon scattering. A (temperature-independent) contribution from defect scattering, which was left out of account theoretically, would make all of the experimental values higher than theory. Al-

TABLE III. Values of the intercept $1/\tau_{e\phi}$ (10^{13} s^{-1}) for the experimental and calculated lines in Figs. 1–3.

| | 78 K | 295 K | 425 K |
|----------|------|-------|-------|
| Cu Expt. | 1.3 | 3.9 | 5.7 |
| Calc. | 1.20 | 2.78 | 3.70 |
| Ag Expt. | 1.5 | 2.2 | 4.5 |
| Calc. | 1.02 | 2.63 | 3.92 |
| Au Expt. | 0.7 | 4.6 | 7.3 |
| Calc. | 1.37 | 3.29 | 4.76 |

TABLE IV. Values of the slope β ($10^{13} \text{ s}^{-1} \text{ eV}^{-2}$) for the experimental and calculated lines in Figs. 1–3.

| | 78 K | 295 K | 425 K |
|----------|------|-------|-------|
| Cu Expt. | 1.9 | 1.9 | 2.4 |
| Calc. | 0.64 | 0.64 | 0.64 |
| Ag Expt. | 1.4 | 1.4 | 1.3 |
| Calc. | 0.73 | 0.73 | 0.73 |
| Au Expt. | 2.2 | 2.4 | 2.5 |
| Calc. | 0.76 | 0.76 | 0.76 |

though most of them are, in fact, somewhat higher, the most obvious discrepancy appears to be an unexpectedly strong temperature dependence of the experimental values for Cu and Au in comparison to the theoretical ones.

The slopes β in Table IV are independent of temperature within the experimental error, as would be expected for the electron-electron scattering mechanism. The numerical values, however, are about 2 times higher for Ag and 3 times higher for Cu and Au, compared to theory,¹⁴ Eq. (5). Thus, while the temperature independence is confirming for the electron-electron mechanism, the quantitative discrepancy between the experimental and theoretical coefficients of $(\hbar\omega)^2$ is a matter of concern, and prompts a comparison with other experimental determinations related to β . The relationships between β and dc transport coefficients are the subject of the next section.

III. RELATIONSHIPS BASED ON ELECTRON-ELECTRON SCATTERING THEORY

In the previous section we have made direct comparison between theory and the optical measurements. In this section we wish to compare our optical data with dc electrical-resistivity and thermal-resistivity data which also show behavior attributed to electron-electron scattering. This comparison is of stronger significance because the theory predicts ratios among various transport coefficients with less uncertainty than the predicted coefficients themselves: All the coefficients contain a basic electron-electron scattering rate $1/\tau_{ee}^0$, which we choose for convenience to be the energy average¹⁵

$$\frac{1}{\tau_{ee}^0} = \int_{-\infty}^{\infty} d\epsilon \left(\frac{-\partial f^0}{\partial \epsilon} \right) \frac{1}{\tau_{ee}^{\text{QP}}(\epsilon)} \quad (7)$$

of the microscopic (quasiparticle) rate $1/\tau_{ee}^{\text{QP}}(\epsilon)$. [$f^0(\epsilon)$ is the equilibrium Fermi function.] The magnitude of this basic scattering rate (7) is one source of considerable uncertainty, but it cancels out when ratios are formed.

Rather general expressions for transport coef-

ficients in terms of τ_{ee}^0 were derived in Ref. 12. Simpler and more transparent expressions were obtained from these in Ref. 4 for the case in which the nonequilibrium electron distribution takes the form

$$\delta f_{\mathbf{k}} = -\vec{u} \cdot \vec{v}_{\mathbf{k}} \tau \left(\frac{\partial f^0}{\partial \epsilon_{\mathbf{k}}} \right), \quad (8)$$

where \vec{u} represents the electric force in the case of the electrical resistivity, or the temperature gradient (actually $\epsilon_{\mathbf{k}} \vec{\nabla} \ln T$) in the case of thermal resistivity. The form (8) is applicable in both sets of experiments of interest here (for different reasons, to be discussed later), and so we quote the relationships from Ref. 4: The dc electrical resistivity is simply

$$\rho_{ee} = \frac{m^* \Delta}{n e^2 \tau_{ee}^0}, \quad (9)$$

and the thermal resistivity

$$W_{ee} = \frac{18 m^* (1 - \langle \cos \theta \rangle + \Delta/2)}{5 \pi^2 n k_B^2 T \tau_{ee}^0} \quad (10)$$

exhibits the electron-electron Lorenz ratio

$$L_{ee} = \frac{\rho_{ee}}{T W_{ee}} = \frac{5 \Delta}{6(1 - \langle \cos \theta \rangle + \frac{1}{2} \Delta)} L_0, \quad (11)$$

where $L_0 = \pi^2 k_B^2 / 3 e^2$ is the "classical" (Wiedemann-Franz law) value. The dimensionless parameter $\langle \cos \theta \rangle$ is defined along with Δ and Γ in Ref. 12; θ is the angle between the two incident velocity vectors in a scattering event.

Finally, the relationship of all this to the intraband absorptivity is expressed by writing the frequency-dependent scattering rate appearing in Eqs. (3) and (5) with more generality in terms of τ_{ee}^0 :

$$\frac{1}{\tau_{ee}(\omega, T)} = \frac{\Delta}{\tau_{ee}^0(T)} \left[1 + \left(\frac{\hbar \omega}{2 \pi k_B T} \right)^2 \right]. \quad (12)$$

The frequency and temperature dependences of Eq. (12) are the same as those of (5) since it is well known that $\tau_{ee}^0(T) \propto T^{-2}$. Furthermore, if τ_{ee}^0 is evaluated as in Refs. 12 and 14 by applying the Born approximation to the Thomas-Fermi screened Coulomb interaction, then (5) is re-

covered with the same numerical values used in Figs. 1-3 and in Table I. However, the validity of the relations (7)-(12) does not depend on any such model of the electron-electron interaction; and so we can make a reasonably model-independent comparison of data from different experiments. Before proceeding to this comparison, we will explicitly outline how one arrives at Eq. (12), starting with Gurzhi's¹¹ original calculation of the frequency- and temperature-dependent conductivity $\sigma(\omega, T)$. This is generally related to the dielectric function $\epsilon(\omega, T)$ by the identity

$$\epsilon = 1 + \frac{4 \pi i}{\omega} \sigma. \quad (13)$$

The conductivity calculation proceeds by solving the time-dependent quantum-mechanical Boltzmann equation iteratively, thus obtaining the distribution function (and conductivity) as an expansion in powers of ω^{-1} . The result is conveniently written as

$$\sigma(\omega, T) = \frac{n e^2}{m^*} \left(\frac{i}{\omega} + \frac{1}{\omega^2 \tau(\omega, T)} + \dots \right), \quad (14)$$

where in Ref. 11 $\tau^{-1}(\omega, T)$ appears as a collision integral. The temperature and frequency dependences of the electron-electron contribution are as given by Eq. (5) (for $\hbar \omega \ll E_F$), but the numerical coefficient was not evaluated quantitatively. However, the integral is formally identical in the $\omega \rightarrow 0$ limit to the collision integral of Ref. 12 [for the case in which (8) applies]. This latter integral is evaluated in terms of the parameters Δ and τ_{ee}^0 (Ref. 16) [Eqs. (2.15)-(2.22) and (2.26) of Ref. 12] and may be written as $1/\tau_{ee}(0, T) = \Delta/\tau_{ee}^0$, leading to Eq. (12). To derive (5), use (2), (3), (12)-(14), and the parametrization^{4,16}

$$1/\tau_{ee}^0(T) = \pi^3 \Gamma (k_B T)^2 / 12 \hbar E_F. \quad (15)$$

We are now prepared to discuss other experiments. The comparisons do not now rely upon any specific model of the electron-electron interaction. They do depend upon the parameters Δ and $\langle \cos \theta \rangle$, which in turn depend on the interaction, but only weakly. (They depend weakly

TABLE V. Electron-electron scattering rate as inferred from optical, dc electrical-, and thermal-conductivity experiments. The fractional umklapp scattering $\Delta < 1$. [$\Delta/(k_B T)^2 \tau_{ee}^0$ ($10^{14} \text{ s}^{-1} \text{ eV}^{-2}$)].

| | Optical conductivity | Low-temperature electrical resistivity | High-temperature Lorenz ratio |
|----|----------------------|--|-------------------------------|
| Cu | 7.5 | 0.74 | 1.6 Δ |
| Ag | 5.5 | 1.0 | 1.7 Δ |
| Au | 9.4 | | 2.6 Δ |

on the *form* of the interaction, but are independent of its magnitude.)

IV. COMPARISON WITH dc TRANSPORT MEASUREMENTS

Our method of comparison with other experiments will be the following: To begin with, we note that the electron-electron contributions to transport coefficients are identified experimentally by their characteristic temperature dependences $\rho_{ee} \propto T^2$ and $W_{ee} \propto T$, both of which originate from the fundamental fact that $\tau_{ee}^0 \propto T^{-2}$. From each transport measurement we may thus try to extract an independent value of $T^2\tau_{ee}^0$. First, we note the optical conductivity value that follows from Eqs. (6) and (12):

$$\frac{\Delta}{(k_B T)^2 \tau_{ee}^0} = 4\pi^2 \beta. \quad (16)$$

The dc electrical-resistivity value of this same quantity follows theoretically from Eq. (9), which is what would also be given by Eq. (12) in the limit $\omega \rightarrow 0$ (even though the analogous correspondence does *not* hold for the electron-phonon contribution). Making use of Eq. (2), we can write

$$\frac{\Delta}{(k_B T)^2 \tau_{ee}^0} = \frac{\omega_p^2}{4\pi(k_B T)^2} \rho_{ee}. \quad (17)$$

Finally, a thermal-conductivity value can be obtained from Eq. (10), or actually from the Lorenz ratio of Eq. (11), in a way that will be explained below in Eq. (18). The last value depends on the calculated umklapp parameter Δ and average scattering angle $\langle \cos \theta \rangle$. The results are collected in Table V. We see that the optical and dc electrical-conductivity results differ by an order of magnitude for Cu and a factor of 5 for Ag. We also see that the thermal results are close to the dc electrical ones for reasonable values of Δ , namely $\Delta = 0.75$ as estimated analytically¹⁴ for all the noble metals or $\Delta = 0.4$ as calculated numerically⁵ for Cu more recently. (The value of $\langle \cos \theta \rangle$ is approximately⁴ -0.35 .) Before drawing our conclusions, however, we must discuss the dc experiments in some detail, since they seek to recover a T^2 contribution that is hidden under other contributions, and this generates some uncertainty.

We consider first the thermal conductivity. The failure of the classical Wiedemann-Franz law for electron-electron scattering, as expressed by Eq. (11), led Laubitz¹⁷ to develop a method for extracting τ_{ee}^0 from combined measurements of both ρ and W at high temperatures (i.e., well above the Debye temperature), where the *electron-phonon* mechanism (if acting alone) would produce

a Lorenz ratio approaching L_0 with increasing temperature. Departures from the Weidemann-Franz law were fit to

$$W - \rho/L_0 T = A/T^2 + BT,$$

with A representing the leading correction due to electron-phonon scattering, and B representing the effect of electron-electron scattering. The theoretical prediction⁴ for B inferred from Eqs. (9) and (10) gives

$$\frac{\Delta}{(k_B T)^2 \tau_{ee}^0} = \frac{5\pi \omega_p^2}{72e^2} B \frac{\Delta}{1 - \langle \cos \theta \rangle - \Delta/3}, \quad (18)$$

where we have again used Eq. (2). The factor $1/(1 - \langle \cos \theta \rangle - \Delta/3)$ depends only weakly on Δ (0.65 ± 0.02 for the Δ values quoted above), so that most of the uncertainty is in the explicit factor Δ . In any case, the discrepancy with the optical values in Table V is probably outside the experimental uncertainty, which is stated¹⁷ to be about 50%. (In the next section, the optical values are shown to have about the same uncertainty.) We note in passing that because the measurements of B are taken at high temperatures, the dominant electron-phonon mechanism may be considered as elastic (on the scale of $k_B T$) and Eq. (8) is therefore a good approximation, as claimed.

The dc electrical-resistivity results that we used, from Khoshnevisan *et al.*,³ involve measurements at very low temperatures in order to escape electron-phonon effects. The temperature-independent electron-impurity effect of course dominates here, requiring very precise measurements; but this ensures once again that Eq. (8) provides a good approximation to the distribution function. Although the dc electrical values are theoretically the most directly comparable with the optical ones, the comparison in Table V should probably still be taken as tentative, for the following experimental reason: A purely electron-electron component in ρ cannot as yet be identified unambiguously in the data. Fitting to the form

$$\rho = \rho_0 + CT^N,$$

Khoshnevisan *et al.*³ find $N \approx 4$ at higher temperatures ($2 \text{ K} < T < 7 \text{ K}$), dropping toward but never quite reaching the expected value 2 at lower temperatures (which extend down to 64 mK for Cu and 30 mK for Ag). For ρ_{ee}/T^2 in Eq. (17) we used the values of C that were tabulated³ for the lowest temperature regions (in which $N \approx 2.03$ for Cu and 2.19 for Ag). We did not try to estimate the difference from the coefficient of a pure T^2 dependence which might presumably be found at still lower temperatures, but it seems clear that

the discrepancy with the optical results is real, especially since the dc electrical results seem to be consistent with the thermal ones.

We conclude this section with references to recent theoretical developments that bear on the identification of the high-temperature optical-frequency conductivity of Eqs. (12) and (16) with the low-temperature dc conductivity of Eqs. (9) and (17). In the latter case, the conductivity can be affected by the fact that electrons interact through the exchange of virtual phonons (as in the superconducting interaction), describable as a frequency- and temperature-dependent renormalization of the Coulomb interaction that is felt in the dc case at low temperatures, but is ineffective at either high frequencies or high temperatures (compared with the Debye frequency or temperature, respectively). This problem has been discussed,^{8,18,19} most recently by MacDonald⁸ with a quantitative estimate of the effect in the noble metals. According to MacDonald the electron-electron contribution to the dc electrical resistivity should vary as T^2 for sufficiently high or low temperatures but not in the intermediate range, and so the coefficient of T^2 should be different in the high- and low-temperature limits. For Cu and Ag MacDonald predicts a reduction in ρ_{ee}/T^2 at low temperatures, from which one would expect the scattering rate inferred from the low-temperature dc ρ_{ee} in Eq. (17) to be less than that from the high-temperature optical parameter β in Eq. (16) as is, in fact, seen in Table V. Unfortunately, however, the magnitude of the effect is much too small (5% and 15%, respectively) to explain the order-of-magnitude discrepancy that we found.

Secondly, there are many-body effects that modify the purely Coulomb part of the electron-electron interaction.^{5,7} These may significantly affect the magnitude of τ_{ee}^0 , but not its temperature dependence nor the values of Δ and $\langle \cos\theta \rangle$. Kukkonen's calculation⁶ incorporates the effects of the compressibility sum rule and core polarization on the electron-electron interaction, but when our values of $\delta\epsilon_1$ for the noble metals are used in the core polarization corrections (to τ_{ee}^0 or ϵ_2), there is little net effect¹ on the resulting values of τ_{ee}^0 . More recently, MacDonald and Geldart⁷ predicted a scattering rate nearly twice as large. (Interestingly, if the most recent values^{5,7} of both Δ and τ_{ee}^0 are combined, the effects nearly cancel, leaving the theoretical prediction about midway between the measured dc and optical results.) In any case, however, this refinement does not alter the predicted relationships of Eqs. (16)–(18) between the measured quantities, so that the discrepancies in Table V are still unexplained.

Finally, we have considered the fact that the optical measurements, unlike the dc ones, sample electronic states which are removed from the immediate vicinity of the Fermi level. To estimate the magnitude of their effect, we have corrected the T and ω dependence of Eq. (5) to allow for first and second derivatives of the density of states $\rho(\epsilon)$ at the Fermi level. We find corrections proportional to $\omega^2 T^2$ and ω^4 , but the magnitudes [within the free-electron model for $\rho(\epsilon)$] are insignificant compared to the ω^2 term.

V. DISCUSSION AND CONCLUSIONS

We showed in Sec. II that the optical scattering rate agreed, in its frequency dependence, with what is predicted by electron-electron scattering theory to within a factor of 2 or 3, a margin that could be accommodated by the experimental and theoretical uncertainties of the quantitative results. In Sec. III, however, it was shown that the same theory, without the assumption of a specific model that would yield absolute magnitudes, predicts general relationships to dc transport processes. Such comparisons were made in Sec. IV, with the result that the optical scattering rate differed from the values derived from dc experiments by as much as an order of magnitude, independently of any specific model of the electron-electron interaction. Since the optically derived rate is greater than the dc one, and could therefore include contributions from other scattering mechanisms in addition to electron-electron scattering, attribution of the optical rate solely to electron-electron scattering (within the framework of current theory) must rest on reconciling the optical and dc experiments. The dc values depend on taking small differences between large quantities, but we can accept as reasonable the authors' estimates of less than 50% uncertainty. The uncertainties in our optical values arise from measurements of very small transmittance and absorbance, and the propagation of the errors through a fairly long set of computations. Thus further discussion of their uncertainty will be worthwhile.

The representative error bars shown in Figs. 1–3 were explained in Ref. 1. An alternative discussion of the optical errors can be based on the absorbance A that is calculated back from our derived parameters $\delta\epsilon_1$, ω_p , and β . This has the advantage that a direct comparison can be made with the reflectance $R = 1 - A$ measured at normal incidence on opaque specimens, including results reported from other laboratories; some such comparisons were illustrated in Ref. 1, Figs. 5–7. The discussion can be analytic in a quad-

ratio approximation that is fairly good¹ up to about 2-eV photon energy:

$$A \cong \frac{2}{\omega_p \tau} \left(1 + \frac{1}{2} (3\delta\epsilon_1 + 1) \frac{\omega^2}{\omega_p^2} \right).$$

With

$$1/\tau = 1/\tau_{e\phi} + 1/\tau_{ee},$$

where $1/\tau_{e\phi}$ is independent of frequency (and for the purpose of this argument can include the defect-scattering rate if that is significant), and

$$1/\tau_{ee} = \beta (\hbar\omega)^2,$$

we have, in the quadratic approximation,

$$A = A_0 + \left(\frac{3\delta\epsilon_1 + 1}{2\omega_p^2} A_0 + \frac{2\hbar^2\beta}{\omega_p} \right) \omega^2,$$

where $A_0 = 2/\omega_p \tau_{e\phi}$. We write the result in this form, treating A_0 as an empirical parameter, in order to show how the frequency variation of the directly measurable quantity A depends on $\delta\epsilon_1$, ω_p , and β . To see how errors in these quantities affect the result, let us assume at first that the frequency dependence of A is exactly determined experimentally, i.e., $d(A - A_0) = 0$; then

$$\frac{1}{2} (3\delta\epsilon_1 + 1) dA_0 + \frac{3}{2} A_0 d(\delta\epsilon_1) + 2\hbar^2 \omega_p d\beta - [(3\delta\epsilon_1 + 1)A_0 + 2\hbar^2 \omega_p \beta] \frac{d\omega_p}{\omega_p} = 0.$$

With our values for Au at room temperature, this becomes

$$7.2 dA_0 + 0.015 d(\delta\epsilon_1) + 0.114 \times 10^{-13} d\beta - 0.42 \frac{d\omega_p}{\omega_p} = 0,$$

assuming $A_0 = 0.01$. From the spread in the results obtained by different investigators, we shall take $dA_0 = 0.005$, $-d\omega_p/\omega_p = 0.05$. It is difficult to obtain a reliable independent estimate²⁰ for $\delta\epsilon_1$, but if we assume $d(\delta\epsilon_1) = 2$, then for Au $|d\beta| < 0.8 \times 10^{13} \text{ s}^{-1} \text{ eV}^{-2}$ in the worst case. The result for Cu is the same, and for Ag the number is 0.5. Now, considering the reasonably good agreement among a variety of measurements of $R = 1 - A$ (see Figs. 5-7 of Ref. 1), we believe our optical β values could not be too large by more than about 50%. Therefore we conclude that our optical results could not be so small as the dc results, which are about an order of magnitude smaller.

If the optical experiments cannot be reconciled with the dc ones, then additional optical scattering mechanisms must be sought that could lead to a scattering rate with the observed frequency and temperature dependence. An interaction of electrons with surface plasmons has recently

been proposed by Sievers.²¹ A resulting plasmon-assisted photon absorption (distinct from the direct absorption by surface plasmons mediated by surface roughness) can explain²¹ the structure in the Drude region of the alkali metals. Although this mechanism is temperature independent, it leads to an initial ω^4 dependence of the Drude scattering rate within the weak-coupling model considered by Sievers. This model is therefore inconsistent with our data on the noble metals (except possibly for the observed upturn in Ag at the highest frequencies in Fig. 2). However, there is no known reason why Sievers's weak-coupling model should necessarily apply to the noble metals, and so we cannot rule out the general mechanism. A judgment on this would require a microscopic theory of the electron-surface plasmon interaction, which presently does not exist.

Another kind of explanation, one which can lead to quadratic frequency dependence, is a two-carrier model,²² which could be appropriate, for example, for the effective conductivity of an inhomogeneous medium composed of crystalline grains and disordered intergranular material.²³ Our films were rather fine grained, since they were evaporated at high rates ($>100 \text{ \AA/s}$) in order to achieve smoothness, but x-ray diffraction showed peak widths² that were limited by the instrumental slit width, indicating average grain size greater than about 400 \AA in the films. Assuming grain boundaries about 10 \AA wide, the volume fraction of disordered material would be less than 5% (for our film thicknesses of less than 500 \AA). The formula derived by Nagel and Schnatterly²³ does, in fact, give an effect comparable to our observed one for 5% disordered material, although it could be much smaller if the electron density is less or the effective mass greater in the disordered regions, contrary to their assumption. (We note that the simple effect of grain-boundary scattering is already included in our analysis.) In any case, they pointed out that this kind of explanation is structure sensitive.

The structure sensitivity of the optical result is a crucial question, and one that cannot yet be resolved on available evidence. Resolution depends on estimating the reliability of the measurement techniques as well as the presumed structure of the samples. Of the accessible data quoted in Ref. 1, some were from single crystals. Among other thin-film data, Thèye's "best" Au film,²⁴ discussed by Nagel and Schnatterly,²³ showed a value of β about one-half to one-third of ours, and her less perfect films showed larger β values, indicating a structure dependence. Thèye's work is probably the most thorough pre-

vious study of this problem. A principal difference from our work is the photon energy range over which the data were analyzed: 0.5–1.1 eV (Thèye) versus 0.6–1.8 eV (present). Although Thèye does not give a detailed error analysis, it will be seen from our figures and those in Ref. 1 that the scatter of these data would preclude drawing any certain conclusions solely within Thèye's more limited range, which is only one-third as large on the ω^2 scale. (On the other hand, the higher-energy data could possibly be contaminated by unknown band-tailing effects.) Another difference is that her film thicknesses and evaporation rates were smaller than those that gave reliable results for us in the interband region. For these reasons we hesitate to accept that Thèye's "best" value of β is definitely smaller than ours; nevertheless, it raises an important problem: Can reliable optical measurements on sufficiently perfect samples be made that the β value proves to be small enough to be consistent with the dc measurements?

VI. SUMMARY

The frequency-dependent contribution to the Drude scattering rate obtained from optical measurements shows the quadratic frequency dependence and temperature independence expected from electron-electron scattering, in all of the noble metals. Although the absolute values agree with theory within tolerable limits, they are up to an order of magnitude larger than the values of the electron-electron contribution in-

ferred from measured dc electrical and thermal resistivities. The combined sources of error in all three types of measurements are apparently not large enough to account for the discrepancy between the optical and dc measurements. The comparisons among the three measured quantities are relatively model independent, in that the rather uncertain theoretical magnitude of electron-electron scattering rate cancels out. We have also discussed refinements to the simple theory (Sec. IV) that might change the predicted relationships between measured quantities, but none of these has a decisive effect for the noble metals. Our conclusion is that the full ω^2 dependence cannot be attributed to electron-electron scattering, at least within the framework of current theoretical understanding. In the search for other mechanisms for our observations, we have discussed (Sec. V) the interaction of electrons with surface plasmons, and the structure dependence as considered in Ref. 23. The former appears doubtful as an explanation because of its predicted frequency dependence. In any case, definitive conclusions would seem to require further experimental and theoretical work.

ACKNOWLEDGMENT

The authors gratefully acknowledge support from the National Science Foundation (G.R.P.), the Department of Energy (W.E.L.), and the National Aeronautics and Space Administration (R.W.C.).

- ¹R. T. Beach and R. W. Christy, *Phys. Rev. B* **16**, 5277 (1977).
²G. R. Parkins, Ph.D. thesis, Dartmouth College, Hanover, New Hampshire, 1978 (unpublished); available from University Microfilms, Ann Arbor, Michigan.
³M. Khoshnevisan, W. P. Pratt, P. A. Schroeder, and S. D. Steenwyk, *Phys. Rev. B* **19**, 3873 (1979); also, above authors and C. Uher, *J. Phys. F* **9**, L1 (1979).
⁴W. E. Lawrence, in *Thermal Conductivity*, edited by V. V. Mirkovich (Plenum, New York, 1978), Vol. 15, p. 197.
⁵J. E. Black, *Can. J. Phys.* **56**, 708 (1978).
⁶C. A. Kukkonen and J. W. Wilkins, *Phys. Rev. B* **19**, 6075 (1979).
⁷A. H. MacDonald and D. J. W. Geldart, *J. Phys. F* **10**, 677 (1980).
⁸A. H. MacDonald, *Phys. Rev. Lett.* **44**, 489 (1980).
⁹T. Holstein, *Ann. Phys. (N.Y.)* **29**, 410 (1964).
¹⁰T. Holstein, *Phys. Rev.* **96**, 535 (1954).
¹¹R. N. Gurzhi, *Zh. Eksp. Teor. Fiz.* **35**, 965 (1958) [Sov.

- Phys.—JETP* **8**, 673 (1959)]; Ph.D. thesis, Institute of Physics and Technology, Academy of Sciences, Ukr S. S. R., Khar'kov, 1958 (unpublished).
¹²W. E. Lawrence and J. W. Wilkins, *Phys. Rev. B* **7**, 2317 (1973).
¹³J. E. Nestell and R. W. Christy, *Am. J. Phys.* **39**, 313 (1971).
¹⁴W. E. Lawrence, *Phys. Rev. B* **13**, 5316 (1976).
¹⁵The energy-averaged rate (7) is related to the quasi-particle scattering rate at the Fermi surface ($\epsilon=0$) by $1/\tau_{ee}^0 = 4/3\tau_{ee}^{QP}(0)$. The chosen energy average is appropriate to the transport coefficients we discuss here.
¹⁶If consulting Ref. 12, the reader will note that the basic electron-electron rate τ_0^{-1} introduced there is related to the present one by $\tau_0^{-1} = 3/2\pi^2\tau_{ee}^0 = 2/\pi^2\tau_{ee}^{QP}(0)$.
¹⁷M. J. Laubitz, *Phys. Rev. B* **2**, 2252 (1970).
¹⁸A. I. Akhiezer, A. I. Akhiezer, and V. G. Baryakhtar, *Phys. Lett.* **44A**, 323 (1973).
¹⁹C. A. Kukkonen and A. W. Overhauser, *Phys. Rev. B* **20**, 550 (1979).

²⁰From the Drude expression, Eq. (3), a plasma resonance ($\epsilon_1 = 0$) is predicted at $\omega = \omega_p / (1 + \delta\epsilon_1)^{1/2}$. This is well known in Ag (but not observable in Cu or Au); the observed resonance energy of about 3.8 eV leads to $\delta\epsilon_1 = 4.6$. Because this value is affected by the interband tail, however, we prefer to use the value $\delta\epsilon_1 \approx 2$ obtained from the infrared and visible measurements.

²¹A. J. Sievers, Phys. Rev. B 22, 1600 (1980).

²²J. J. Hopfield, in *Superconductivity in d- and f-Band Metals, Rochester*, Proceedings of the Conference on Superconductivity in d- and f-Band Metals, edited by D. H. Douglas (American Institute of Physics, New York, 1972), p. 358.

²³S. R. Nagel and S. E. Schnatterly, Phys. Rev. B 9, 1299 (1974).

²⁴M. L. Thèye, Phys. Rev. B 2, 3060 (1970).